LETTER

doi:10.1038/nature13131

Dynamic sensory cues shape song structure in *Drosophila*

Philip Coen[1,2], Jan Clemens[1,2], Andrew J. Weinstein[1,2], Diego A. Pacheco[1,2], Yi Deng[3]† & Mala Murthy[1,2]

The generation of acoustic communication signals is widespread across the animal kingdom[1,2], and males of many species, including Drosophilidae, produce patterned courtship songs to increase their chance of success with a female. For some animals, song structure can vary considerably from one rendition to the next[3]; neural noise within pattern generating circuits is widely assumed to be the primary source of such variability, and statistical models that incorporate neural noise are successful at reproducing the full variation present in natural songs[4]. In direct contrast, here we demonstrate that much of the pattern variability in *Drosophila* courtship song can be explained by taking into account the dynamic sensory experience of the male. In particular, using a quantitative behavioural assay combined with computational modelling, we find that males use fast modulations in visual and self-motion signals to pattern their songs, a relationship that we show is evolutionarily conserved. Using neural circuit manipulations, we also identify the pathways involved in song patterning choices and show that females are sensitive to song features. Our data not only demonstrate that *Drosophila* song production is not a fixed action pattern[5,6], but establish *Drosophila* as a valuable new model for studies of rapid decision-making under both social and naturalistic conditions.

Drosophila melanogaster males chase females during courtship and produce song by wing vibration; females, meanwhile, arbitrate mating decisions. We developed a behavioural chamber to record acoustic signals and fly movements simultaneously (Fig. 1a and Supplementary Video 1); fly movements provide information on the sensory cues that may influence song production. We collected a large data set (>100,000 song bouts) to model the relationship between sensory cues and song patterning. Most experiments involve females that are pheromone-insensitive[7] and blind (termed PIBL) to facilitate auditory response measurements. All fly types used are described in Extended Data Table 1.

For one wild-type strain (WT1), we show that using arista-cut (deaf) females or wing-cut (mute) males increased the time to copulation and decreased the percentage of mated pairs (Fig. 1c). This corroborates prior work[8,9] demonstrating the importance of song for courtship success. Pairing WT1 males with wild-type, rather than PIBL, females did not alter these results (Fig. 1c), nor any of the results described below (not shown). All wild-type strains showed similar success with PIBL females (Extended Data Fig. 1b). Courtship songs comprise two modes (sine and pulse; Fig. 1b) and are part of a genetically hardwired mating ritual, thought to be stereotyped[6,10]. However, we find frequent mode transitions and variable mode durations individualize song bouts (Fig. 1d and Extended Data Fig. 2).

Males spend approximately 20% of courtship time singing (Extended Data Fig. 1c), and bouts can begin with either song mode. Using reverse correlation, we found that all tracking parameters correlate with bout initiations (Extended Data Fig. 3). We therefore turned to the generalized linear model (GLM) (Fig. 2a), widely used to analyse binary response data with several explanatory variables[11–13]. Unlike reverse correlation[14], the GLM we use includes a sparsity prior, which disentangles the contributions of correlated parameters to song patterning (see Methods)—this represents a major difference between our approach and previous studies[15].

Given similarities across fly strains (Extended Data Fig. 3), we combined data from all wild-type flies (315 pairs, 84,904 song bouts) for GLM analyses. We selected the most predictive features (≤ 600 ms of tracking parameter history) for each model based on deviance reduction (Extended Data Fig. 4a, b). For pulse song starts, combining two features: male forward velocity (mFV) and male lateral speed (mLS) strongly improved model fit (Fig. 2b). When tested on separate data, the fraction of correctly classified song starts (*P*Cor) was 0.67 (Fig. 2c), representing a 34% improvement over the null model (*P*Cor = 0.5). This compares favourably with fMRI-based predictions of human behaviour[16]

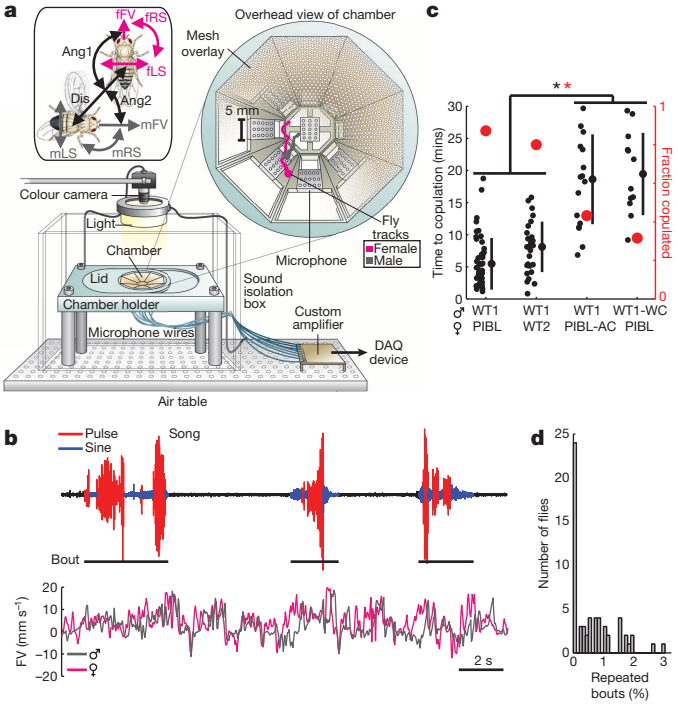

Figure 1 | A novel assay to study *Drosophila* song behaviour. a, Behavioural chamber with tracked fly movements (see Methods). Fly movements are divided into: male/female forward velocity (mFV/fFV), male/female lateral and rotational speeds (mLS/fLS and mRS/fRS), the distance between fly centres (Dis), the absolute angle from female/male heading to male/female centre (Ang1/Ang2). **b**, Segmentation of song bouts into pulse (red) and sine (blue) elements (top). Corresponding traces for mFV and fFV (bottom). **c**, Song is important for mating. Time to copulation increases (black, $*P < 0.001$) and fraction of copulated pairs decreases (red, $*P < 0.01$) when females are deaf or males are mute. Individual points, mean, and s.d. are given for each genotype ($n = 35$–48 pairs). AC, arista cut; WC, wing cut. **d**, Song is variable. The number of repeated bouts (containing pulse and sine) per fly (see Methods). $n = 60$ wild-type males.

[1]Princeton Neuroscience Institute, Princeton University, Princeton, New Jersey 08544, USA. [2]Department of Molecular Biology, Princeton University, Princeton, New Jersey 08544, USA. [3]Department of Physics, Princeton University, Princeton, New Jersey 08544, USA. †Present address: Department of Biophysics, University of Washington School of Medicine, Seattle, Washington 98195, USA.

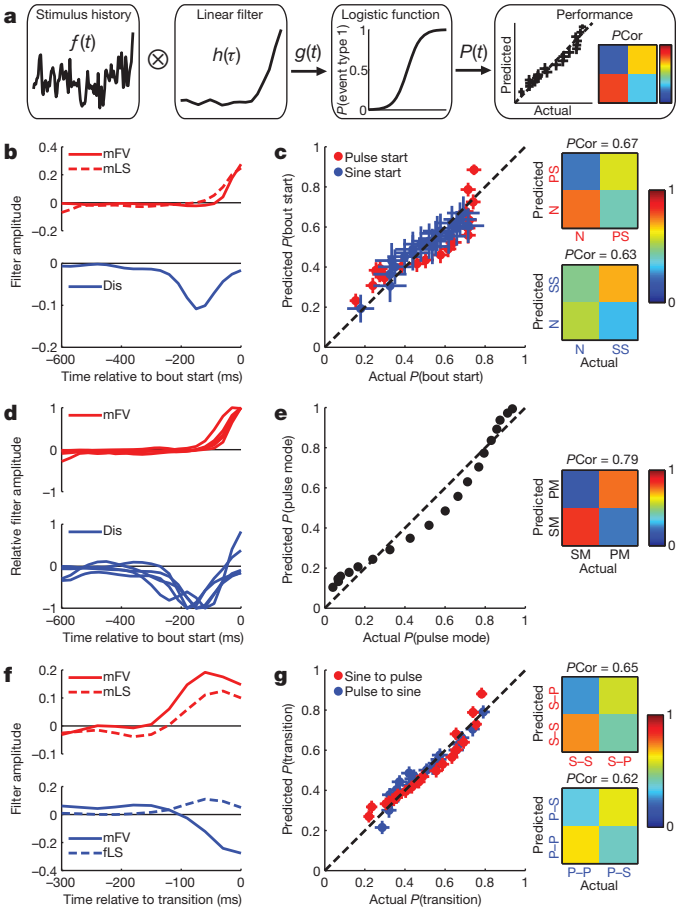

Figure 2 | Song bout patterning is predictable and based on few features. **a**, Schematic of the GLM (see Methods). Inputs—stimulus histories (features; $f(t)$) for each movement parameter—are used to predict binary event probabilities. Significant features are convolved with a linear filter $h(\tau)$, and the result, $g(t)$, is transformed into a probability $P(t)$, via a logistic function. Performance plots show the predicted and actual event probability relationships. Confusion matrices, from which we derive *P*Cor values, quantify model performance. **b**, Filters for pulse and sine song initiation GLMs. Unlike male lateral speed (mLS) or male forward velocity (mFV), the Dis filter indicates a time lag between distance estimation and sine song initiation. **c**, GLM performance for identifying pulse song starts (PS) using male forward velocity and male lateral speed filters ($n = 11{,}020$ test events from 315 males) and sine song starts (SS) using the Dis filter ($n = 2{,}476$ test events from 315 males). N = no song start. **d**, Male forward velocity pulse song start filters and Dis sine song start filters are similar for data from pheromone-insensitive or arista-cut males or males paired with arista-cut or sex-peptide-injected females; filters from wild-type males are also plotted. **e**, GLM performance for classifying current song mode (PM, pulse mode; SM, sine mode) using mean male forward velocity and male lateral speed ($n = 55{,}464$ test events from 315 males). **f**, Filters for sine to pulse (S–P) transitions (top) and the pulse to sine (P–S) transitions (bottom). **g**, GLM performance for identifying S–P transitions (versus continued sine song (S–S)) using male forward velocity and male lateral speed filters ($n = 17{,}118$ test events from 315 males) and P–S transitions (versus continued pulse song (P–P)) using male forward velocity and female lateral speed filters ($n = 11{,}748$ test events from 315 males). Error bars (most too small to visualize) indicate 95% confidence intervals (**c**, **e**, **g**).

and with two-alternative forced choice behavioural performance in *Drosophila*[17]. *P*Cor values are equivalent ($r^2 = 0.98$) to area under the curve values, an alternative performance measure (Extended Data Fig. 4c, d). We used a similar GLM framework to identify female forward velocity (fFV) as the best predictor of changes in male motion (male forward velocity (Extended Data Fig. 5a–c) and male lateral speed (data not shown)): that is, when the female speeds up, the male accelerates to follow her. Therefore, any correlation between male motion and song mode choice ultimately establishes a link between a sensory cue (for example, female motion) and song patterning. We address this point further below.

For songs that start in sine mode, the optimal model included only the distance between fly centres (Dis) (Fig. 2b, c and Extended Data Fig. 6a). Song start filters derived from PI (pheromone-insensitive) or arista-cut males paired with PIBL females, or from wild-type males paired with arista-cut or unreceptive/sex-peptide-injected[18] (SP) females, were indistinguishable from wild-type filters (Fig. 2d), even though males take longer to copulate with arista-cut females (Fig. 1c), and never copulate with unreceptive/sex-peptide-injected females (Extended Data Fig. 7a). A model designed to distinguish song bouts beginning in sine versus pulse mode retains male forward velocity and the distance between fly centres as the most predictive features, but with significantly increased performance (Extended Data Fig. 6b, c). Therefore, we focus hereafter on song patterning decisions, rather than the male's decision to sing versus perform another courtship behaviour. Here a decision refers to a behavioural choice biased by sensory information[19].

During song bouts, males typically alternate between sine and pulse modes, with each mode lasting tens to hundreds of milliseconds. We next investigated whether GLMs could also predict the current mode of song within bouts. Model performance was optimal using only two features: male forward velocity and male lateral speed (a 58% improvement over the null model; Fig. 2e). The absence of the distance between fly centres (Dis) feature in this model is probably due to its reduced variance during song (Extended Data Fig. 6d, e). Using different, male-centric, features only decreased model performance (Extended Data Fig. 8). We then went on to predict all mode transitions within a bout: increases in male forward velocity and male lateral speed predict transitions to pulse mode, whereas decreases in male forward velocity and increases in female lateral speed predict transitions to sine mode (Fig. 2f). Mode transitions represent a subtle change in behaviour (for example, whether 300 ms of pulse song is followed by 30 ms of sine song or 30 ms of continued pulse song); nonetheless, our model predictions produced a combined *P*Cor of 0.64 (Fig. 2g). Thus, taking into account male motion and inter-fly distance can largely explain variability in song patterning. Although studies in birds have shown that auditory cues, either produced by the singer itself[20] or by a duetting partner[21], affect acoustic sequence generation, to our knowledge, ours is the first demonstration of a role for non-auditory sensory inputs in dynamically patterning the structure of individual song sequences.

Next, we considered which sensory pathways mediated the male's decision-making during song production. Although male motion is the primary contributor to song patterning in our models, we observed a strong correlation ($r^2 = 0.95$) during song bouts between inter-fly distance (beyond the tactile range of ~5 mm; the tail of the distribution in Extended Data Fig. 6d) and the pulse/sine ratio (Fig. 3a; correlation is independent of male movement). We conclude that flies use vision to measure distance over this range, because blind males or wild-type males placed in the dark, sing significantly more pulse song (Fig. 3b, c); this is not true for any other sensory deficit and cannot be explained by changes in male speed (Extended Data Fig. 5e).

Previous studies have demonstrated that separate neurons control pulse and sine song production[22,23]. This indicates that song patterning is neurally controlled, and does not arise simply from mechanical coupling with male locomotion changes. In support of this, males sing both song modes at all velocities (Fig. 3d). We further conclude that visual measurements of optic flow are not used to convey male motion signals to song patterning networks, because a model based on only male forward velocity and male lateral speed predicts current song mode for blind males (Fig. 3e). This left two likely possibilities (Fig. 3f): either (mechanism 1) a cue from the female induces males to change speed and concomitantly affects song patterning or (mechanism 2) neural circuits that carry information about male motion (via either a copy of the motor commands or proprioceptive feedback from the legs) modulate song patterning circuits. Because female forward velocity predicts

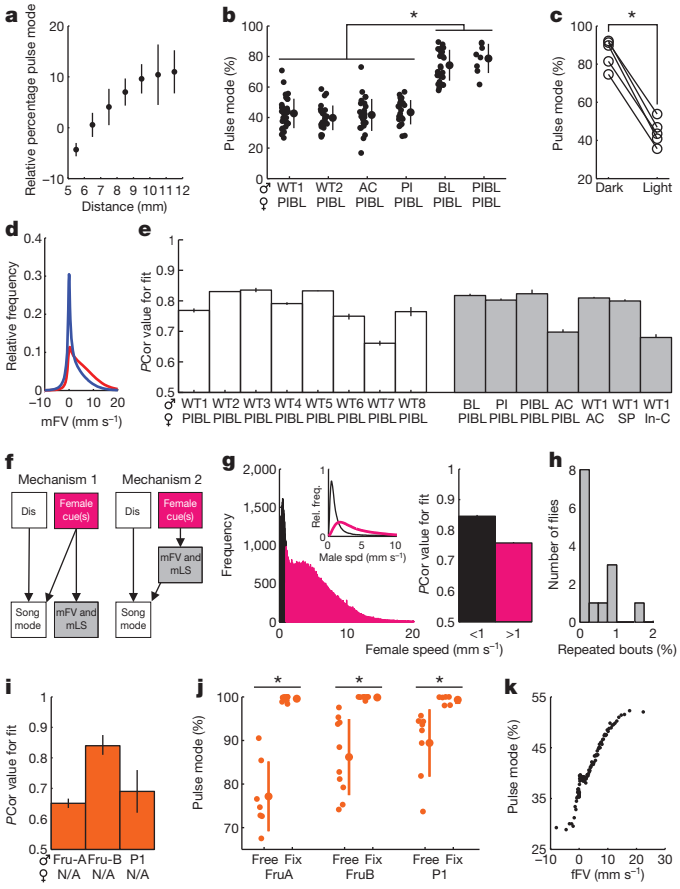

Figure 3 | Neural pathways that modulate song patterning. **a**, Percentage of song in pulse mode (mean and s.d.) increases with inter-fly distance ($r^2 = 0.95$; see Methods). **b**, Pulse song percentage increases in blind males ($n = 11$–48 flies, $^*P < 0.001$). **c**, Individual WT2 males (paired with PIBL females) produce more pulse song in dark versus light ($n = 5$ flies, $^*P < 0.0001$). **d**, Normalized event frequency for pulse or sine song (red or blue, $n = 57{,}0225$ or $n = 95{,}2541$, from 315 males) at each male forward velocity, across all wild-type strains. **e**, *P*Cor values from classifying current song mode (using mean male forward velocity and male lateral speed) for wild-type strains (white bars) and various sensory manipulations ($n = 924$–16,256 test events from 11–48 flies for each model). **f**, Two potential neural circuit mechanisms underlying the correlation between male motion and song. Female cue(s) directly modulate both song patterning and locomotor circuits (left) or circuits carrying information about male motion (right) modulate song patterning circuits. **g**, Wild-type data were split into songs produced when females were not moving or moving (left, black or magenta, $n = 9{,}454$ or $n = 46{,}204$, test events from 315 males; see Methods). Inset shows corresponding male speeds. Corresponding *P*Cor values from classifying current song mode using mean male forward velocity and male lateral speed (right). **h**, Song variability with TrpA1-activated flies ($n = 14$ males from 3 genotypes) is similar to wild type (Fig. 1d). **i**, *P*Cor values from classifying current song mode using mean mFV and mLS for Fru-A, Fru-B, and P1-activated males ($n = 1{,}987$ and 200 and 100 test events from 7 and 10 and 8 males, respectively). **j**, For each genotype, the percentage of pulse song increases ($^*P < 0.01$) when flies are fixed. **k**, Correlation between female forward velocity and the percentage of pulse song ($n = 16{,}092$ from 315 wild-type males paired with PIBL females, binned by percentile) at a 60 ms lag ($r^2 = 0.91$). Error bars indicate 95% confidence intervals (**e**, **g**, **i**). **b** and **j** show individual data points, mean and s.d. for each group.

male motion (Extended Data Fig. 5a–c), song patterning would ultimately be dependent on sensory cues for both mechanisms.

To distinguish between these mechanisms, we removed the link between female cues and male motion. Male lateral speed and male forward velocity still predicted current song mode when males are pheromone-insensitive and/or blind (Fig. 3e). Given that blind males do not follow females (Extended Data Fig. 5d), and produce song over a wide range of inter-fly distances/orientations (Extended Data Fig. 8d–g), it seems unlikely that a non-visual, long-range cue from the female patterns song in these males. Further, model performance remains high when females provide no motion cues (Fig. 3g and Extended Data Fig. 9). Finally, we examined the link between male motion and song patterning without a female present. We artificially activated song and targeted three neural subsets (see Methods). For all genotypes, levels of inter-bout variability were similar to wild-type levels despite constitutive thermal activation (Fig. 3h). Again, male lateral speed and male forward velocity predicted current song mode (Fig. 3i) within the performance range for wild-type strains (Fig. 3e). By preventing these males from moving, we observed a marked reduction in sine song (Fig. 3j); because this song mode is typically produced at lower male speeds, our results indicate that a copy of the locomotor commands (presumably still active in 'fixed' males) is more likely (than proprioceptive feedback) to pattern song. Thus, our data support the conclusion that activity in locomotor circuits influences song patterning, favouring mechanism 2 (Fig. 3f). Consistent with this, we observed the strongest correlation ($r^2 = 0.91$) between female forward velocity and the pulse/sine ratio in wild-type flies at the delay at which males follow females (Fig. 3k and Extended Data Fig. 5b).

As a final test of the importance of sensory cues in song patterning, we considered song bout terminations. The exponential distribution of syllable durations in songbirds has been proposed to support a stochastic mechanism for syllable termination[24]. Bout durations in *Drosophila* are also well fit by an exponential function ($r^2 = 0.98$; Extended Data Fig. 2). However, we identified female lateral speed as a significant predictor of bout ends (Fig. 4a, b). We posit that when males sense changes in female lateral speed they either transition to sine song (Fig. 2f) or they end song altogether.

On the basis of the data presented, we propose that, for *Drosophila*, detection of a female[25] gates the song production pathway. Once gated, sensory cues act directly (inter-fly distance and female lateral speed) or indirectly (via male forward velocity and male lateral speed) to pattern song on short timescales (Fig. 4c). Although trial-to-trial variability in acoustic signals may be useful for song learning in birds[26], *Drosophila* males do not learn their songs. Therefore, we considered alternative roles for patterning decisions in fly mating behaviours. Because female speed decreases before copulation (Fig. 4d), we reasoned that female slowing was a sign of receptivity. Indeed, using the GLM framework, we found a negative correlation between the amount of either song mode, in a given time window, and female speed (Fig. 4e). This relationship was reduced for deaf females, whereas unreceptive (SP) females showed a positive correlation between speed and song amount, a reversal of wild-type behaviour. In addition, females increased or decreased speed in response to song from *Drosophila simulans* (heterospecific) or WT1 (conspecific) males, respectively. This is particularly striking when considering that, for the same experiment, male motion predicts song mode choice for both *D. simulans* and *D. melanogaster* males (Fig. 4f). Therefore, male song patterning choices are unlikely to be used by females for mate selection. Indeed, successful males (those that copulated within 30 min) and unsuccessful males pattern song similarly (Extended Data Fig. 7b–d). We speculate that males bias towards their louder form of song (pulse) when far from the female (captured by the distance between fly centres feature) or when trying to catch up to, or locate, the female (captured by the male forward velocity and male lateral speed features); this would maximize the probability of the female hearing his song and decreasing her locomotion. It remains to be determined, however, over which specific distances and angles females can detect each song mode (and amplitude modulations therein).

In conclusion, instinctive behaviours, like acoustic signal production, have been generally considered to comprise a series of fixed action patterns, elicited and oriented by sensory information[27]. Courtship song production in *Drosophila* has long been regarded as an example of such a fixed action sequence[5,6], with the female serving as the trigger stimulus. In contrast to this view, we show that even the simple fly uses sensory

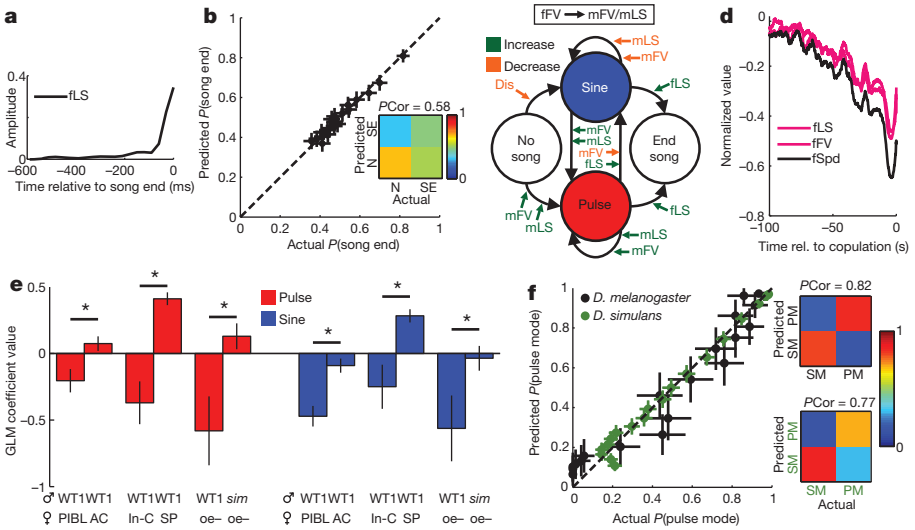

Figure 4 | Song patterning decisions and female responses. **a**, Filter from GLM for song ends. **b**, GLM performance for identifying song ends (SE) using female lateral speed ($n = 10{,}708$ events from 315 males). N, no song end. **c**, Summary of the influence of sensory inputs on song patterning, as revealed by GLM analysis. **d**, Normalized changes in female motion before copulation ($n = 233$ flies). **e**, GLM coefficient values between pulse or sine song density and female speed (*$P < 0.01$, $n = 40$ to $n = 1{,}429$ samples from 7–38 pairs; see Methods). **f**, GLM performance for classifying current song mode using mean male forward velocity and male lateral speed for WT2 or *sim* (black or green, $n = 1424$ or 9854 test events from 31 or 40 flies) males paired with oe- (oenocyte-less and PIBL) females. Error bars are 95% confidence intervals (**b**, **e** and **f**).

information to pattern his song sequences over short timescales. These data therefore offer a new window into the study of instinctive behaviours, and indicate that song production in flies may be more analogous to complex motor behaviours, such as prey capture, known to rely heavily on sensory feedback for patterning. More broadly, and consistent with recent studies of fly flight and human mobility[28,29], we suspect that seemingly stochastic behaviours may be more predictable than expected.

METHODS SUMMARY

Behavioural data (song and video recordings) were acquired by pairing virgin male and female flies in a custom-built chamber, designed to capture fly acoustic signals throughout the environment (~25 mm diameter, tiled with 9 microphones and connected to a specialized amplifier[30]) and to be compatible with our fly tracking software. Male wild-type strains came from diverse geographic locations; most females tested were genetically engineered to be both blind (*GMR-hid*) and pheromone-insensitive (*orco*). Other genetic and physical manipulations included arista cutting (deaf flies), wing cutting (mute males), sex-peptide-injection and oenocyte removal. Neural activation was achieved by expressing TrpA1 in three different subsets of Fru^{+} neurons and heating the entire chamber before introduction of male flies. All data processing and analysis was conducted in MATLAB. Song was segmented as previously described[30]. A modified generalized linear model[11], which uses a sparseness prior in order to penalize redundant features, was implemented to determine whether fly movements and positions could predict male song patterning choices, including bout initiation, song mode (pulse versus sine) within a bout, mode transitions and bout termination. When fitting or testing models over 1,000 iterations, data were randomly subsampled to equalize the frequency of each event type (a common method for dealing with uneven event frequencies). Predictive features for each model were selected using deviance reduction and model performance was tested using independent data sets. *P*Cor values were used to quantify model performance. To measure female responses to song, female speed and amount of male song were compared using a 1 min sliding window, with 50% overlap.

Online Content Any additional Methods, Extended Data display items and Source Data are available in the online version of the paper; references unique to these sections appear only in the online paper.

Received 11 June 2013; accepted 5 February 2014.
Published online 5 March 2014.

1. Doupe, A. J. & Kuhl, P. K. Birdsong and human speech: common themes and mechanisms. *Annu. Rev. Neurosci.* **22,** 567–631 (1999).
2. Bentley, D. & Hoy, R. R. The neurobiology of cricket song. *Sci. Am.* **231,** 34–50 (1974).
3. Sakata, J. T. & Brainard, M. S. Online contributions of auditory feedback to neural activity in avian song control circuitry. *J. Neurosci.* **28,** 11378–11390 (2008).
4. Jin, D. Z. & Kozhevnikov, A. A. A compact statistical model of the song syntax in Bengalese finch. *PLoS Comput. Biol.* **7,** e1001108 (2011).
5. Hall, J. C. The mating of a fly. *Science* **264,** 1702–1714 (1994).
6. Demir, E. & Dickson, B. J. *fruitless* splicing specifies male courtship behavior in *Drosophila*. *Cell* **121,** 785–794 (2005).
7. Ziegler, A. B., Berthelot-Grosjean, M. & Grosjean, Y. The smell of love in *Drosophila*. *Front. Physiol.* **4,** 72 (2013).
8. von Schilcher, F. The role of auditory stimuli in the courtship of *Drosophila melanogaster*. *Anim. Behav.* **24,** 18–26 (1976).
9. Bennet-Clark, H. C. & Ewing, A. W. Pulse interval as a critical parameter in the courtship song of *Drosophila melanogaster*. *Anim. Behav.* **17,** 755–759 (1969).
10. Baker, B. S., Taylor, B. J. & Hall, J. C. Are complex behaviors specified by dedicated regulatory genes? Reasoning from *Drosophila*. *Cell* **105,** 13–24 (2001).
11. Mineault, P. J., Barthelme, S. & Pack, C. C. Improved classification images with sparse priors in a smooth basis. *J. Vis.* **9,** http://dx.doi.org/10.1167/9.10.17 (2009).
12. Calabrese, A., Schumacher, J. W., Schneider, D. M., Paninski, L. & Woolley, S. M. A generalized linear model for estimating spectrotemporal receptive fields from responses to natural sounds. *PLoS ONE* **6,** e16104 (2011).
13. Pillow, J. W. *et al.* Spatio-temporal correlations and visual signalling in a complete neuronal population. *Nature* **454,** 995–999 (2008).
14. Sharpee, T., Rust, N. C. & Bialek, W. Analyzing neural responses to natural signals: maximally informative dimensions. *Neural Comput.* **16,** 223–250 (2004).
15. Trott, A. R., Donelson, N. C., Griffith, L. C. & Ejima, A. Song choice is modulated by female movement in *Drosophila* males. *PLoS ONE* **7,** e46025 (2012).
16. Soon, C. S., Brass, M., Heinze, H. J. & Haynes, J. D. Unconscious determinants of free decisions in the human brain. *Nature Neurosci.* **11,** 543–545 (2008).
17. Perisse, E. *et al.* Different Kenyon cell populations drive learned approach and avoidance in *Drosophila*. *Neuron* **79,** 945–956 (2013).
18. Yapici, N., Kim, Y. J., Ribeiro, C. & Dickson, B. J. A receptor that mediates the post-mating switch in *Drosophila* reproductive behaviour. *Nature* **451,** 33–37 (2008).
19. McFarland, D. J. Decision making in animals. *Nature* **269,** 15–21 (1977).
20. Sakata, J. T. & Brainard, M. S. Real-time contributions of auditory feedback to avian vocal motor control. *J. Neurosci.* **26,** 9619–9628 (2006).
21. Fortune, E. S., Rodriguez, C., Li, D., Ball, G. F. & Coleman, M. J. Neural mechanisms for the coordination of duet singing in wrens. *Science* **334,** 666–670 (2011).
22. Ewing, A. W. The neuromuscular basis of courtship song in *Drosophila*: the role of the direct and axillary wing muscles. *J. Comp. Physiol.* **130,** 87–93 (1979).
23. Shirangi, T. R., Stern, D. L. & Truman, J. W. Motor control of *Drosophila* courtship song. *Cell Rep.* **5,** 678–686 (2013).
24. Aronov, D., Veit, L., Goldberg, J. H. & Fee, M. S. Two distinct modes of forebrain circuit dynamics underlie temporal patterning in the vocalizations of young songbirds. *J. Neurosci.* **31,** 16353–16368 (2011).
25. Dickson, B. J. Wired for sex: the neurobiology of *Drosophila* mating decisions. *Science* **322,** 904–909 (2008).
26. Olveczky, B. P., Andalman, A. S. & Fee, M. S. Vocal experimentation in the juvenile songbird requires a basal ganglia circuit. *PLoS Biol.* **3,** e153 (2005).
27. Tinbergen, N. *The Study of Instinct* (Clarendon Press, 1951).

28. Censi, A., Straw, A. D., Sayaman, R. W., Murray, R. M. & Dickinson, M. H. Discriminating external and internal causes for heading changes in freely flying *Drosophila*. *PLoS Comput. Biol.* **9,** e1002891 (2013).
29. Song, C., Qu, Z., Blumm, N. & Barabasi, A. L. Limits of predictability in human mobility. *Science* **327,** 1018–1021 (2010).
30. Arthur, B. J., Sunayama-Morita, T., Coen, P., Murthy, M. & Stern, D. L. Multi-channel acoustic recording and automated analysis of *Drosophila* courtship songs. *BMC Biol.* **11,** 11 (2013).

Supplementary Information is available in the online version of the paper.

Acknowledgements We thank B. Arthur and D. Stern for assistance in establishing the song recording system; P. Andolfatto for wild-type fly strains; S. Kamal and V. Cheng for assistance with selecting and maintaining fly strains; G. Guan for technical assistance; T. Tayler for help with injections; J. Shaevitz for help with the fly tracker; R. da Silveira for early discussions on reverse correlation; and G. Laurent, C. Brody, D. Aronov, I. Fiete, M. Ryan, and the entire Murthy lab for thoughtful feedback and comments on the manuscript. Figure 1a was illustrated by K. Ris-Vicari. P.C. is funded by an HHMI International Predoctoral Fellowship and M.M. is funded by the Alfred P. Sloan Foundation, the Human Frontiers Science Program, an NSF CAREER award, the McKnight Endowment Fund, and the Klingenstein Foundation.

Author Contributions P.C. and M.M. designed the study. P.C., A.J.W. and D.A.P. collected and processed the data. Y.D. developed the fly tracking algorithm. P.C. and J.C. analysed the data. P.C. and M.M. wrote the paper.

Author Information Reprints and permissions information is available at www.nature.com/reprints. The authors declare no competing financial interests. Readers are welcome to comment on the online version of the paper. Correspondence and requests for materials should be addressed to M.M. (mmurthy@princeton.edu).

METHODS

Fly strains and rearing. For all experiments, we used 3–7-day-old virgin flies. All flies were raised in density-controlled bottles seeded with 8 males and 8 females for 4 days. Bottles were kept at 25°C and 60% relative humidity. Virgin flies were then housed individually and kept in behavioural incubators (TriTech) under 12 h/12 h light/dark cycling. Male flies were 'painted' with a small spot of opaque ultraviolet-cured glue (Norland Electronic Adhesives) on the dorsal mesothorax to facilitate identification during tracking.

All wild-type strains, except for the laboratory colony Canton-S (WT2), were supplied by the Andolfatto group at Princeton University. These strains descended from single females caught in geographically diverse locations (see Extended Data Table 1). For several experiments, we used genetically modified flies. All genetic mutations were recombined into the Canton-S genetic background; their genotypes are: PIBL (pheromone-insensitive and blind): w^+/w^+; *GMR-hid/+; orco*$^-$*/orco*$^-$; oe- (oenocyte-less and PIBL): *GMR-hid/+; PromE800-Gal4, Tub-Gal80ts/UAS-hid,UAS-stingerII; orco*$^-$*/orco*$^-$; PI (pheromone-insensitive): w^+/w^+;+/+; *orco*$^-$*/orco*$^-$; BL (blind): w^+/w^+; *GMR-hid/GMR-hid*; Fru-A (TrpA1 expressed in all *fruitless*-positive neurons): *UAS-TrpA1/sco; fru*^{P1}*-GAL4/TM6B*; Fru-B (TrpA1 expressed in mostly brain-specific *fruitless*-positive neurons): *tsh-Gal80/UAS-TrpA1; fru*^{P1}*-GAL4/TM6B*; P1 (TrpA1 expressed in P1 song command neurons): *NP2631/UAS-frtstopfrt-TrpA1; fru* ^{P1}*-FLP/TM6*B.

We acquired *GMR-hid* flies from the Bloomington Stock Center, *PromE800-Gal4, Tub-Gal80ts; UAS-hid, UAS-stingerII* flies from J. Levine, *orco*− flies from L. Vosshall, *fru* ^{P1}-GAL4 and *fru* ^{P1}*-FLP* from B. Dickson, and NP2631 from the Kyoto stock centre. For arista- and wing-cutting paradigms (AC and WC), to render flies deaf (AC) or mute (WC), WT1 flies were anaesthetized with CO_2, and aristae or wings were removed, with fine forceps, over 20 h before recording. *Drosophila melanogaster* sex peptide[31] or a control peptide (SIFamide[32]) were injected into PIBL virgin females 12–24 h before recording. These flies were anaesthetized on ice during injections.

Recording apparatus. The recording chamber (Fig. 1a) is octagonal and covered in a layer of copper mesh; the chamber itself was milled from white delrin by Schmit Prototypes (Menomonie, WI). The floor is sloped at an angle such that the effective chamber diameter is 25 mm (~10 fly body lengths); this is large enough to permit a range of fly motions and interactions (Supplementary Video 1). Using sloped chamber sides facilitates fly tracking[33]. The lid was made from clear plexiglass. The floor of the chamber is tiled with 9 NR23158 microphones (Knowles Electronics) to capture male song throughout the chamber. Each microphone connects to a custom-built amplifier[30]. The open areas around the microphones increase signal-to-noise ratio. The entire chamber is enclosed inside an acrylic box—with a door for loading flies—and placed on an air table to minimize microphone noise. The camera for recording fly movement, a Unibrain 540c with a Fujinon HF16HA-1B lens, was suspended above the acrylic box, and a DigiSlave L-Ring 3200 LED light was used to illuminate the behavioural chamber. Room lighting was off during all recordings.

Courtship assay. Before the first recording of each day, the chamber was prepared in two steps. First, the underside of the cover glass was rinsed and coated with Sigmacote (Sigma-Aldrich) to prevent flies from walking on the chamber ceiling. Second, to odourize the environment, >4 flies (strain WT2) were placed inside the chamber for 10 min. Flies were loaded individually into the chamber using a custom-built aspirator. To optimize for peak fly activity, we began recordings within 150 min of the behavioural incubator lights switching on. Recordings were terminated when copulation occurred or after 30 min (classified as 'no copulation'). Recordings with no song in the first 5 min (excepting the WC paradigm) were terminated early and disregarded. Data from flies that moved < 1.5 mm per minute, or sang at low amplitudes relative to other flies of the same strain, were excluded on the basis of possible poor health (this criteria applied to 25/679 males).

Dark/light transition assay. For acute transitions between dark/light conditions (see Fig. 3c), the chamber was covered completely with BK5 Blackout Fabric (Thor Labs), and flies were loaded in darkness using a Spot 90-Lumen LED headlamp (Black Diamond) on the red light setting. After 10 min of courtship in the dark, the LED L-Ring light was switched on. If flies copulated in the dark then the trial was disregarded.

Thermogenetic activation experiments. For thermogenetic activation of Fru-A, Fru-B, and P1 neurons in males (no female in the chamber), the chamber was heated with a coil (HSTAT, BriskHeat) to 25 °C (for FruA activation), 27 °C (for FruB activation), or 32 °C (for P1 activation). In the 'Fix' condition, each fly's legs were fixed in place with UV-curable glue. Songs from these males were segmented as described above, except that the criteria for bout, pulse, and sine identification were relaxed to account for small differences between heat-activated and naturally produced song (for example, increased variability in inter-pulse interval). Song from both freely moving and fixed flies were analysed with the same modified criteria.

Data processing and analysis. All data processing and analysis was conducted in MATLAB (MathWorks).

Significance testing. Unless otherwise specified in the text, significance tests were as follows:

To determine significant differences between means, we used one-way ANOVA or Kruskal–Wallis analyses, depending on whether the distributions in question were non-normal (as identified by the Jarque-Bera test for normality). For confidence intervals, both for model selection and in Fig. 4e, non-overlap was used as a conservative estimate of significant differences. For normally distributed data, variance was estimated to be similar between groups, as required for applying ANOVA. Given variability in behaviour, we sampled a large number of flies for each wild type strain (~40) before performing any statistical tests. After observing the effect size in wild type data, we then collected between 5 and 40 flies (depending on the analysis) for other genotypes and manipulations. Blinding was not necessary for these experiments because all data analyses were automated. As all statistical tests were performed between different fly strains (with the exception of Fig. 3c, for which there is an internal control), randomization of animal groups was not necessary.

Fly tracking and song segmentation. Fly positional tracking was achieved by optimizing (for flies) an algorithm originally developed for tracking bacteria[34]. Tracking errors occurred at a low rate (~1 switch in fly identity or orientation every 25 or 12 min, respectively) and were corrected manually using custom software. We performed song segmentation using automated software[30]. We combined segmentation results from the 9 microphones into a single song with false positive and negative rates similar to those reported in ref. 30. Audio (10 kHz) and video (30 Hz) sampling frequencies were synchronized using a Master 8 (A.M.P.I.), to simultaneously drive an LED and buzzer.

Quantification of movement parameters. Males can approach the female from either side during courtship. As a result, distinctions between left/right lateral movement and anticlockwise/clockwise rotations or angles are not meaningful for the analyses we performed. For this reason, only forward velocities were allowed to take negative vales and we use absolute values for lateral movements and rotations. It should be noted that the relative contributions of forward and lateral movements to song patterning could be better established with a faster video frame rate.

Quantifying the percentage of repeated bouts. Bouts were down-sampled to 50 Hz (from 10 kHz). This temporal resolution was chosen to approximate the fastest pulse rate in fly song; events on this timescale are likely to have ethological significance. Mixed bouts (containing both sine and pulse trains) were converted into strings of ones (sine) and zeros (pulses) at the 50 Hz sampling rate. For males singing more than 100 mixed bouts of song, we calculated the number of repeated bouts to be: 1 − (number of unique binary strings/total number of binary strings). Therefore, a 'percentage of repeated bouts' of zero for a fly indicates that no two mixed bouts produced by this fly had the same pulse/sine patterning, when sampled at 50 Hz.

Analysing song statistics. For Extended Data Fig. 2a–k, only mixed bouts (those containing both sine and pulse elements) were included in analyses. Empirical joint probability density functions (PDFs) were calculated by binning data in 2 dimensions. Independent PDFs were calculated as the outer product of the empirical marginal PDFs. For bout durations (Extended Data Fig. 2e, f), only bouts shorter than 2 s were included in PDF estimation due to the sparsity of the matrix beyond this cutoff. The kernel density estimates seen in Extended Data Fig. 2l were calculated using the ksdensity function in MATLAB.

Bout triggered averages (BTAs). Given the difference between audio/video sampling rates, we resampled relevant sections of our tracking data, keeping the sampling rate the same (30 Hz) but aligning motion samples with song bout onset. For each movement parameter, we subtracted the mean between 3 s and 2.5 s before song initiation; subtracting the mean of the entire courtship session (many minutes) instead artificially increased variability, as some flies had long periods of quiescence when not singing. Mean-subtracted trials were aligned and averaged to calculate BTAs shown in Extended Data Fig. 3.

GLM implementation. For all models, data were first split into groups hereafter termed 'fitting data' (66%) and 'testing data' (34%). We fit all models using the method described in ref. 11, which imposes a sparseness-inducing prior on basis coefficients; this method penalizes redundant features. When fitting or testing models over 1,000 iterations, data were randomly subsampled each time to equalize the frequency of each event type (a common method for dealing with uneven event frequencies). For models where we sought to determine the predictive power of a model based on male lateral velocity and male forward velocity, rather than identify the most predictive feature, model selection was not performed. If a model combined data from multiple fly strains, we first *z*-scored movement features for each strain before running the model to account for any genetic differences in behaviour.

Model selection. The fitting procedure for the binomial GLM takes as inputs features (stimulus histories for movement parameters) and binary events associated

with each feature (for example, 'no song start' versus 'song start', encoded as 0 and 1). All stimulus histories are convolved with a linear filter yielding a linear prediction. The filter represents the weight for time points before each event; positive/negative deviations in the filter indicate that an increase/decrease in the stimulus is predictive of event type 1. The linear prediction is then transformed to the predicted event probability using a logistic function. We first fit separate models for each movement feature, repeating each fit 1,000 times (the data were split evenly for fitting and cross-validation) to calculate 95% confidence intervals for the deviance reduction (for example, see Extended Data Fig. 4a, b). If the deviance reduction for a single feature was greater than zero, we then re-ran models with paired inputs (for example, male forward velocity and male lateral velocity), to determine if adding a second feature improved model performance. We continued to add features until the relative improvement from an additional feature was not significantly greater than 10%.

Model performance. We convolved each of the 1,000 filters generated during fitting iterations with the testing data; the convolved data were then passed through a nonlinear logistic function to calculate a probability score for each stimulus history predicting event 1 versus event 0 (see Fig. 2a). For each test, *P*Cor values were calculated by comparing the actual outcome (whether events were type 0 or type 1) with the predicted outcome. A predicted probability >0.5 was counted as an outcome of type 1. Receiver operating characteristic (ROC) curves where generated by varying this 0.5 threshold between 0 and 1 and running the test 1,000 times for each threshold to get estimates of the false positive and true positive rates; AUC statistics were then calculated from these ROC curves. Performance plots were generated by sorting predictions in ascending order and grouping data using 5% intervals and plotting the mean prediction value against the percentage of type 1 events for each of the 20 groups. These plots serve as a visualization tool.

Song start prediction. GLMs were trained to distinguish song starts (either pulse or sine start) from potential song starts. We considered a stimulus history of 600 ms before events, for all features. For potential song starts (times when the male is not singing), we constrained selected time points to those times when Dis <8 mm and Ang2 $<60^{\circ}$, for the entire 600 ms period. We also only included actual song starts that met these criteria (~65% of song starts). These winnowing criteria were only used for models presented in Fig. 2b–d and Extended Data Fig. 8c. As well as song start predictions, we also ran a model to classify between sine and pulse starts, given that a song start had occurred; the goal of this analysis was to eliminate noise arising from unidentified behaviours (such as attempted copulation) that prevent song starts. For this, we used the same stimulus histories described above, but only for times when song starts actually occurred and without applying any winnowing criteria (Extended Data Fig. 6b, c).

Current song mode prediction. GLMs were trained to distinguish pulse mode from sine mode. We extracted movement features during 600 ms of pulse or sine song and considered only the central 300 ms (with a 150 ms buffer either side) of this time window. This prevented contamination of the data with behaviours related to transitions, song ends, or song starts. Temporal information for this model was not relevant, so the GLM was trained and tested using the mean values of each movement feature within the central 300 ms window. Results were not significantly different for models generated using 10 separate time points rather than taking the mean (data not shown). For current song mode models applied to subsets of data, the data set was split before the separation of 'fitting' and 'testing' data. To examine model performance when females were effectively stationary, we split the data into samples when female speed was $<1\ \mathrm{mm\ s^{-1}}$ or $>1\ \mathrm{mm\ s^{-1}}$ (Fig. 3f and Extended Data Fig. 9). Similarly, to examine model performance when blind males were at large distances, or facing away from the female, we split the data into samples when Dis was <5 mm or >5 mm, or Ang2 was $<60^{\circ}$ or $>60^{\circ}$, respectively (Extended Data Fig. 8d–g).

Transition prediction. GLMs were trained to distinguish transitions (pulse-to-sine or sine-to-pulse) from continual song (pulse-to-pulse or sine-to-sine). Due to the fast nature of transitions, we considered 300 ms of stimulus history—this represents half the length considered for song starts or song ends. Song was classified as a transition if there was a switch in mode immediately following this 300 ms window.

Song end prediction. GLMs were trained to distinguish actual song bout ends from potential song bout ends. We included all bout ends with at least 600 ms of song preceding the bout end. Potential song bout ends were considered to be any 600 ms period of song that did not precede the end of a bout.

Male velocity prediction. GLMs were trained to predict male forward velocity values (at time points during male song) using the preceding 600 ms of each of the other 8 movement parameters. Owing to the analogue nature of the output data (male velocities can take a wide range of values), a nonlinear logistic function was not applied to the values after convolving with linear filters. As a result, model performance is demonstrated with the comparison of all predicted and actual male forward velocities (and corresponding r^2 value for the fit), and not with a *P*Cor (Extended Data Fig. 5).

Female response to song. Female speed, along with male song data, were extracted using a sliding window of width 1 min, with 50% overlap. A range of window sizes were tested, but the results were not significantly affected unless windows became smaller than 15 s (data not shown), at which point estimates became too noisy. Time windows within 1 min of fly introduction and less than 1 min before copulation were not used, to eliminate female behaviours relating to initial introduction or copulation. A GLM was used to determine if the amount of pulse or sine song within a window predicted the mean female speed within the same window. Female speed was calculated using only time points within the window >300 ms from any song (sine or pulse), to prevent confounding effects related to male singing decisions. Only windows containing $>5\%$ (some courtship) or $<95\%$ (to allow for speed estimates) song were included.

Effect of distance on pulse/sine ratio. To eliminate the effect of velocity on song patterning (discovered in this study), we binned velocities into 1 $\mathrm{mm\ s^{-1}}$ windows and analysed the relationship between inter-fly distance and the pulse/sine ratio of song within each velocity bin (see Fig. 3a). Owing to the rarity of song at significant inter-fly distances, all wild-type fly strains were combined in this analysis. For each velocity window, we subtracted the mean pulse/sine ratio for all song at that velocity. Thus, negative values indicate that the pulse/sine ratio at that distance was lower than the overall ratio for that velocity. Ratios were only included if 100 song samples existed for a particular velocity/distance combination; means and standard deviations were calculated using all relative ratios that met these criteria at a particular distance. Distances below 5 mm were excluded to eliminate confounding effects of tactile interactions.

Fraction of song in pulse mode. Flies were included in this analysis (see Fig. 3b, c and j) only if they sang more than 25 bouts during the courtship period. For acute dark/light transitions (Fig. 3c), flies were required to sing at least 25 bouts during both dark and light conditions.

Female behaviour before copulation. Data from all wild type strains courting PIBL females were combined for this analysis (see Fig. 4d). Only flies that took longer than 3 min to copulate were included. The first minute of each recording was eliminated to avoid analysing behaviours associated with chamber introduction, and we examined only the 100 s preceding copulation. Each movement parameter was normalized by subtracting the mean value during 120–100 s period before copulation and dividing by the standard deviation within the final 100 s. Data were analysed similar to the BTAs (see above).

31. Yapici, N., Kim, Y. J., Ribeiro, C. & Dickson, B. J. A receptor that mediates the post-mating switch in *Drosophila* reproductive behaviour. *Nature* **451,** 33–37 (2008).
32. Verleyen, P. *et al.* SIFamide is a highly conserved neuropeptide: a comparative study in different insect species. *Biochem Biophys Res Commun.* **320,** 334–341 (2004).
33. Simon, J. C. & Dickinson, M. H. A new chamber for studying the behavior of *Drosophila*. *PLoS ONE* **5,** e8793 (2010).
34. Deng, Y., Coen, P., Sun, M. & Shaevitz, J. W. Efficient multiple object tracking using mutually repulsive active membranes. *PLoS ONE* **8,** e65769 (2013).
35. Senthilan, P. R. *et al. Drosophila* auditory organ genes and genetic hearing defects. *Cell* **150,** 1042–1054 (2012).

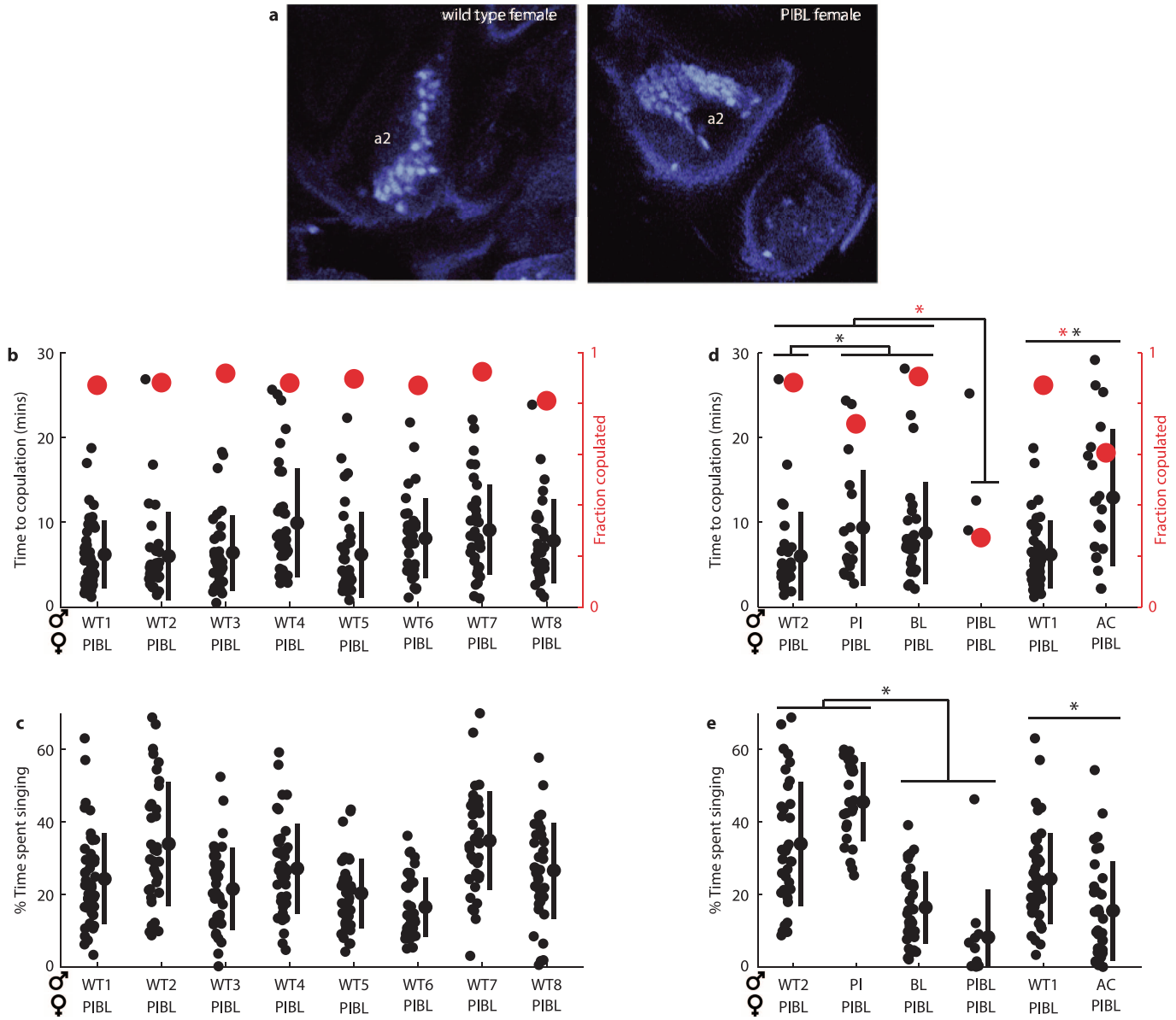

Extended Data Figure 1 | Courtship behaviour with PIBL females. **a**, Recently, genes involved in photoreceptor development have been implicated in JO neuron function[35], so we confirmed that the *GMR*-hid mutation (which induces photoreceptor apoptosis) did not affect JO neuron development. Here we show a single *z* plane image of the antenna of a wild-type (left) or PIBL (right) female fly, labelled with anti-elav (blue) to mark the nuclei of JO neurons. **b,** Time to copulation (black) and fraction of copulating pairs (red) are similar for all 8 wild-type strains. $n = 34–48$ males for each strain. **c,** The percentage of time males spent singing for all 8 wild-type strains. $n = 34–48$ males for each strain. **d,** As in **b**, but for arista cut, pheromone-insensitive, blind and PIBL males compared with wild-type strains of matched genetic background (WT2 for pheromone-insensitive, blind, and PIBL and WT1 for arista cut). $*P < 0.05$, $n = 11–48$ males for each genotype. **e,** As in **c**, but for arista-cut, pheromone-insensitive, blind, and PIBL males compared with wild-type strains of matched genetic background. $*P < 0.01$, $n = 11–48$ males for each genotype. **b–e,** Individual points, mean and s.d. are given for each strain/genotype.

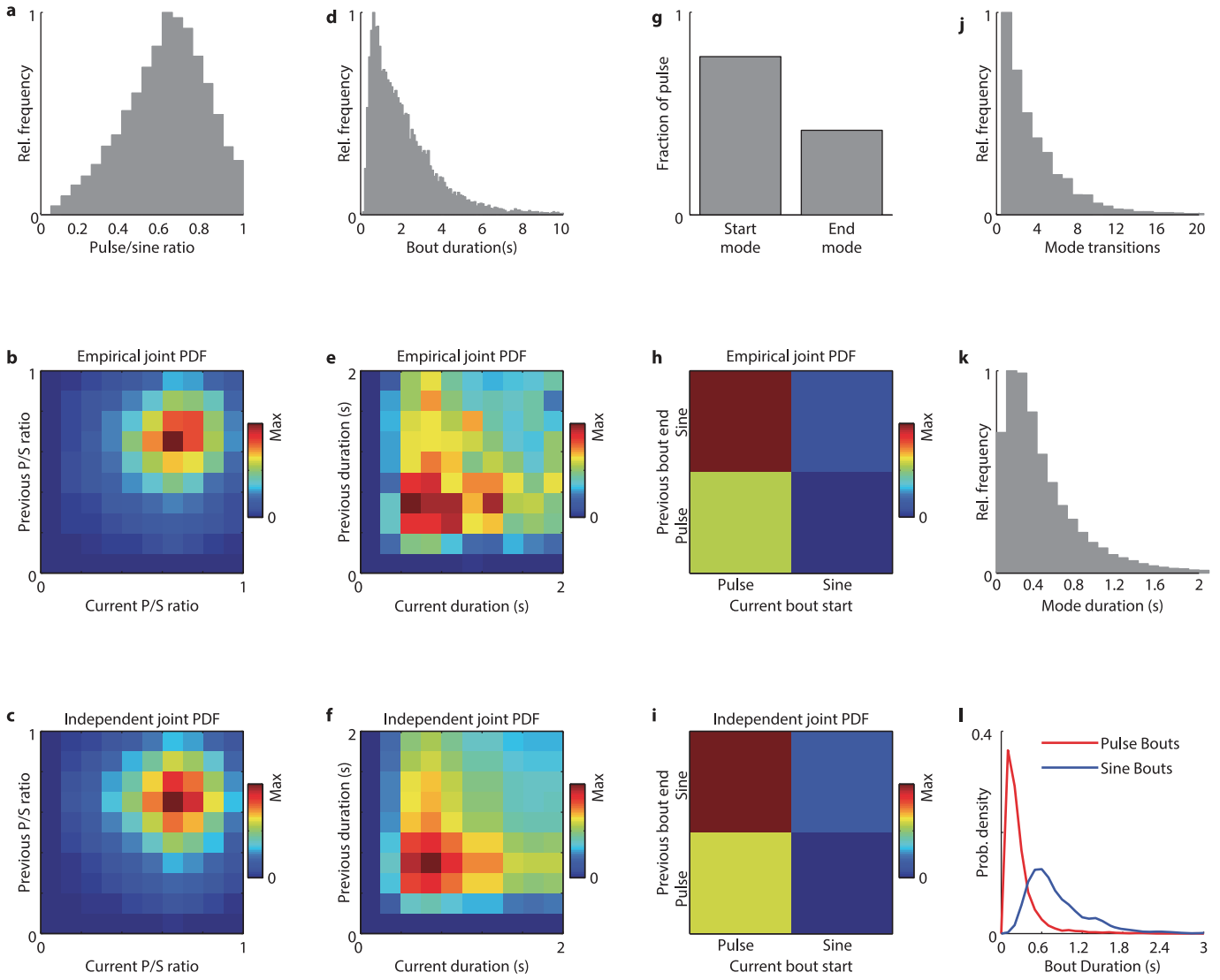

Extended Data Figure 2 | Song bout statistics for wild-type strains courting PIBL females. For all panels, data come from the 116 males singing more than 100 song bouts. **a,** Relative frequency of the pulse/sine ratio for mixed bouts (song bouts containing both sine and pulse elements). $n = 15{,}489$ bouts. **b,** The empirical joint probability density function (PDF) of pulse/sine ratios for consecutive pairs of mixed bouts (see Methods). $n = 10{,}805$ bouts. **c,** As in **b**, but the independent, rather than empirical, joint PDF. The independent joint PDF is given by multiplying the individual 1D distributions of current and previous bouts for each bin within the 2D space. The distributions in **b** and **c** are not significantly different ($P = 0.99$, two-sample Kolmogorov–Smirnov test). **d,** Relative frequency of bout durations for mixed bouts. $n = 15{,}489$ bouts. **e,** The empirical joint PDF of bout durations for consecutive pairs of mixed bouts lasting less than 2 s. $n = 3{,}535$ bouts. **f,** As in **e**, but the independent, rather than empirical, joint PDF. The distributions in **e** and **f** are not significantly different ($P = 0.19$, two-sample Kolmogorov–Smirnov test). **g,** The fraction of mixed bouts starting and ending in pulse mode. $n = 15{,}489$ bouts. **h,** The empirical joint PDF of the ending and starting modes for consecutive pairs of mixed bouts. $n = 10{,}805$ bouts. **i,** As in **h**, but the independent, rather than empirical, joint PDF. The distributions in **h** and **i** are not significantly different ($P = 0.99$, two-sample Kolmogorov–Smirnov test). **j,** Relative frequency of the number of mode (sine or pulse) transitions within mixed bouts. $n = 15{,}489$ bouts. **k,** Relative frequency of the durations of each song mode (sine or pulse) within mixed bouts. $n = 76{,}979$ song modes. **l,** Relative frequency of durations of non-mixed song bouts, comprising a single song mode. $n = 8{,}624$ or n = 772 for pulse only or sine only, respectively.

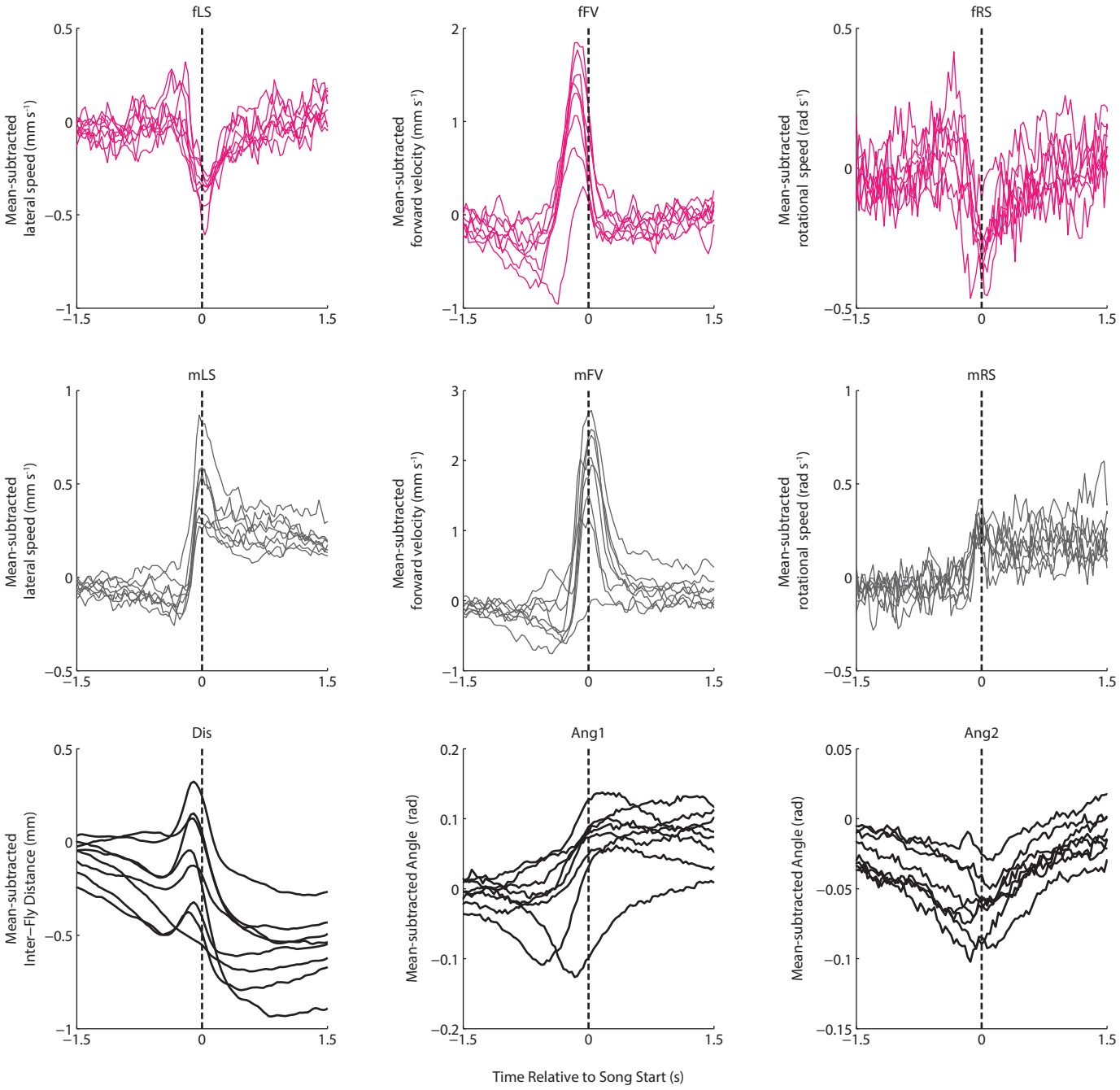

Extended Data Figure 3 | Bout triggered averages (BTAs) for all nine movement parameters for song starts. BTAs are formed similar to spike-triggered averages (STAs) for neural data. Movement parameters for each of the 8 wild-type strains were aligned to the start of song (n = 2,427–7,586 bouts from 34–48 males). All males were paired with PIBL females. Female and male parameters are coloured magenta and grey, respectively. For each trial, movement parameters were mean-subtracted before averaging (see Methods).

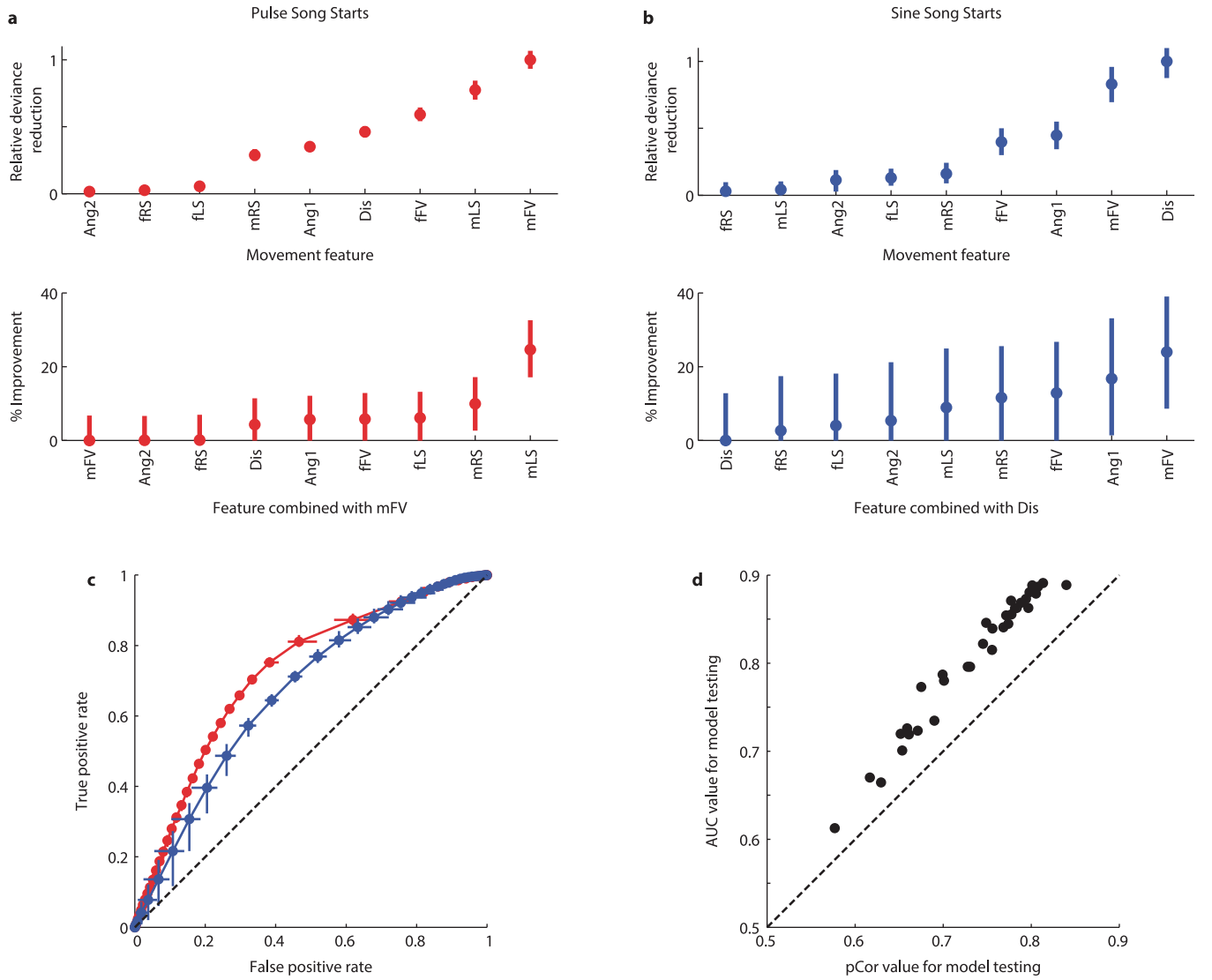

Extended Data Figure 4 | Model selection criteria examples and comparison of model performance statistics. **a,** Top, first, we train nine separate GLMs, each based on a single feature, followed by cross-validation on two-thirds of the data, with 1,000 repetitions. The single feature which gives the greatest reduction in deviance is chosen—here male forward velocity for the detection of song bouts that start in pulse mode. Bottom, a second feature is included in the model if the additional reduction in deviance improves the model by a minimum of 10%—here male lateral speed. **b,** Top, as in **a** but for song bouts that start in sine mode. Dis is selected as the most predictive feature. Bottom, as in **a**, but no second feature results in a significant model improvement, so only the one feature model is used. **c,** Receiver operating characteristic curves for GLM models designed to identify pulse (red) and sine (blue) song starts. Integrating the area under the curve (AUC) shows that both models perform significantly better than chance, for which AUC would be 0.5. AUC = 0.72 (for the pulse starts model) and 0.62 (for the sine starts model). **d,** Comparison between the *P*Cor and AUC values for every model presented in this study, showing a high correlation between the two measures: $r^2 = 0.98$. For every model tested, the *P*Cor value is a more conservative measure of performance. Error bars indicate 95% confidence intervals, although some are too small to visualize (**a–c**).

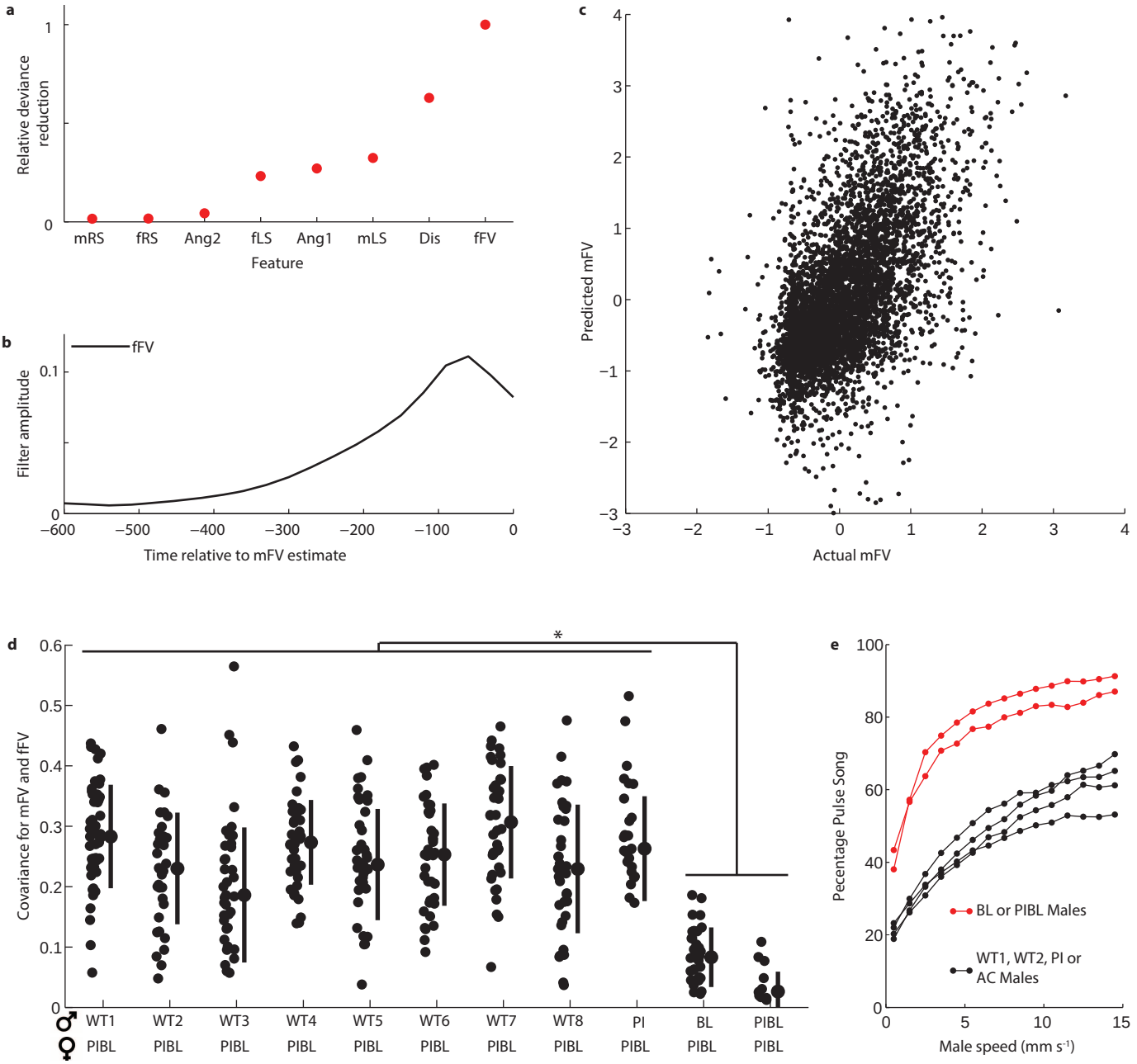

Extended Data Figure 5 | Female forward velocity changes predict male forward velocity changes in wild-type and pheromone-insensitive males, but not blind or PIBL males. **a,** Relative deviance reduction for GLMs, one for each movement feature, to predict male forward velocity at time points during song. Female forward velocity is the optimal predictor. Error bars indicate 95% confidence intervals, although some are too small to visualize. **b,** The female forward velocity linear filter is most predictive of male forward velocity values at a lag of ~60 ms. **c,** GLM performance for predicting male forward velocity based only on female forward velocity ($n = 58{,}1814$ test events from 315 pairs, $r^2 = 0.39$). Values of male forward velocity and female forward velocity were normalized such that $\mu = 0$ and s.d. = 1 (see Methods). A total of 1% of the data (randomly selected) is plotted here for illustrative purposes. **d,** As an estimate of the time males spent following females, we measured the maximum cross-covariance (normalized by the auto-covariance) between male and female forward velocities, $n = 11$–48 males for each strain. Perfect following behaviour, over the entire trial, would produce a value of 1. We tested all following delays between 0 and 300 ms. BL and PIBL, but not PI, males show significantly reduced following compared with all other WT strains, $^*P < 0.05$. Individual points, mean, and s.d. are given for each strain/genotype. **e,** The two blind male genotypes (blind and PIBL, red) sing a higher percentage of pulse song at all male speeds (binned to nearest mm s^{-1}) compared with wild-type males or males with other sensory manipulations (WT1, WT2, pheromone-insensitive, and arista-cut, black). In all cases, females were PIBL. Speeds > 15 mm s^{-1} were excluded owing to insufficient data. For each point, $n = 1{,}208$–15,736 samples.

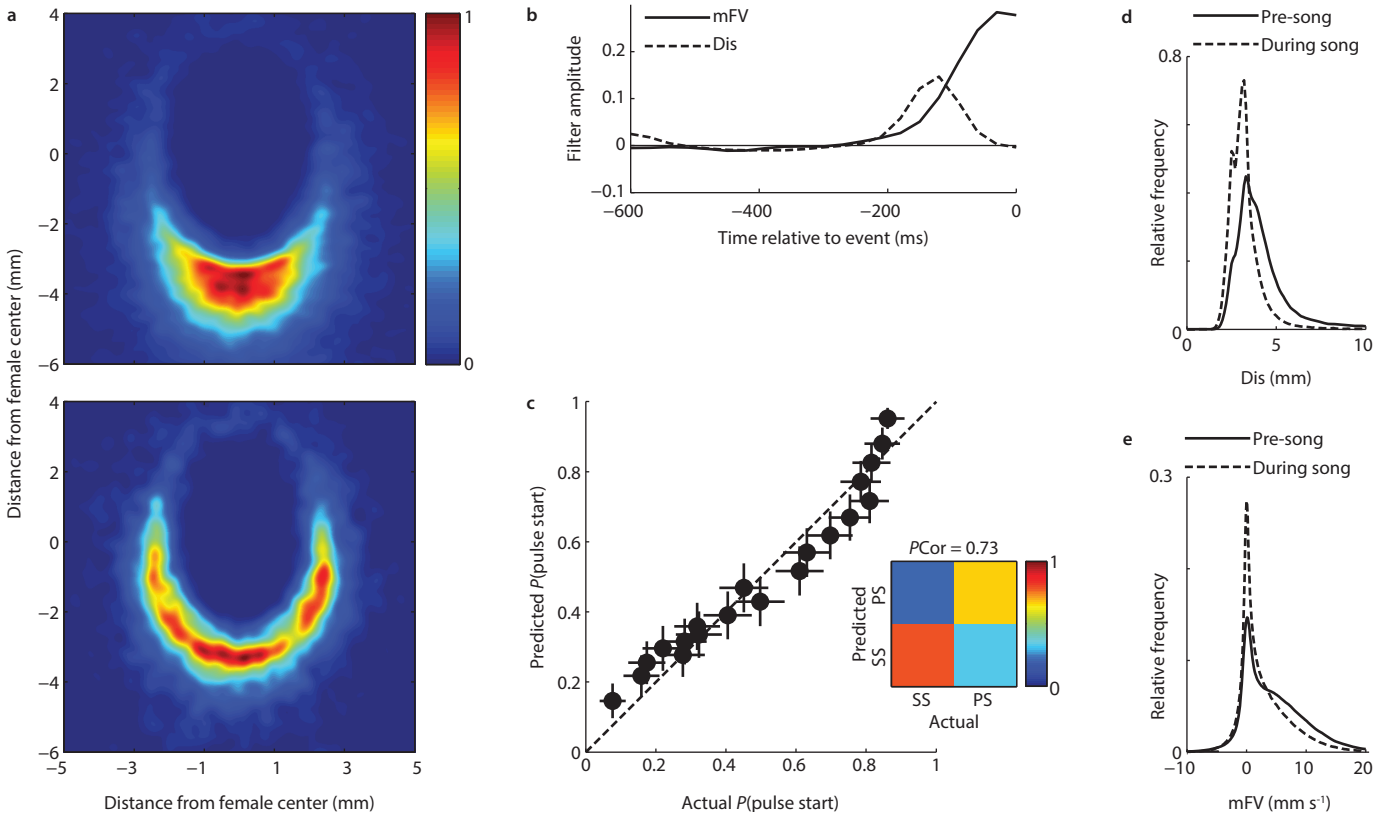

Extended Data Figure 6 | Relationships between male–female distance, male velocity and song bout starts. **a,** A two-dimensional normalized kernel density estimate of the male centre relative to the female centre (0,0) at the time of song bout initiation using combined data from all wild-type males. Males are positioned further from the female when they start a song bout in pulse mode (top, $n = 27{,}820$ bouts from 315 males) versus sine mode (bottom, $n = 5{,}749$ bouts from 315 males). **b,** Linear filters for male forward velocity and Dis, the most predictive features for the song start mode classification GLM (predicting sine song starts (SS) versus pulse song starts (PS)). **c,** GLM performance for classifying song start mode with male forward velocity and Dis filters ($PCor = 0.73$, $n = 3{,}904$ test events from 315 males). Error bars indicate 95% confidence intervals. **d,** Relative frequency distribution of Dis for periods 150 ms before the start of song bouts (solid) and during song (dashed), $n \geq 20{,}1414$ time points from 315 males. The variance in Dis is larger, by 229%, for time points before song. **e,** As in **d**, but for male forward velocity. The variance increase in male forward velocity for time points before song is 58%, much smaller than the increase observed with Dis.

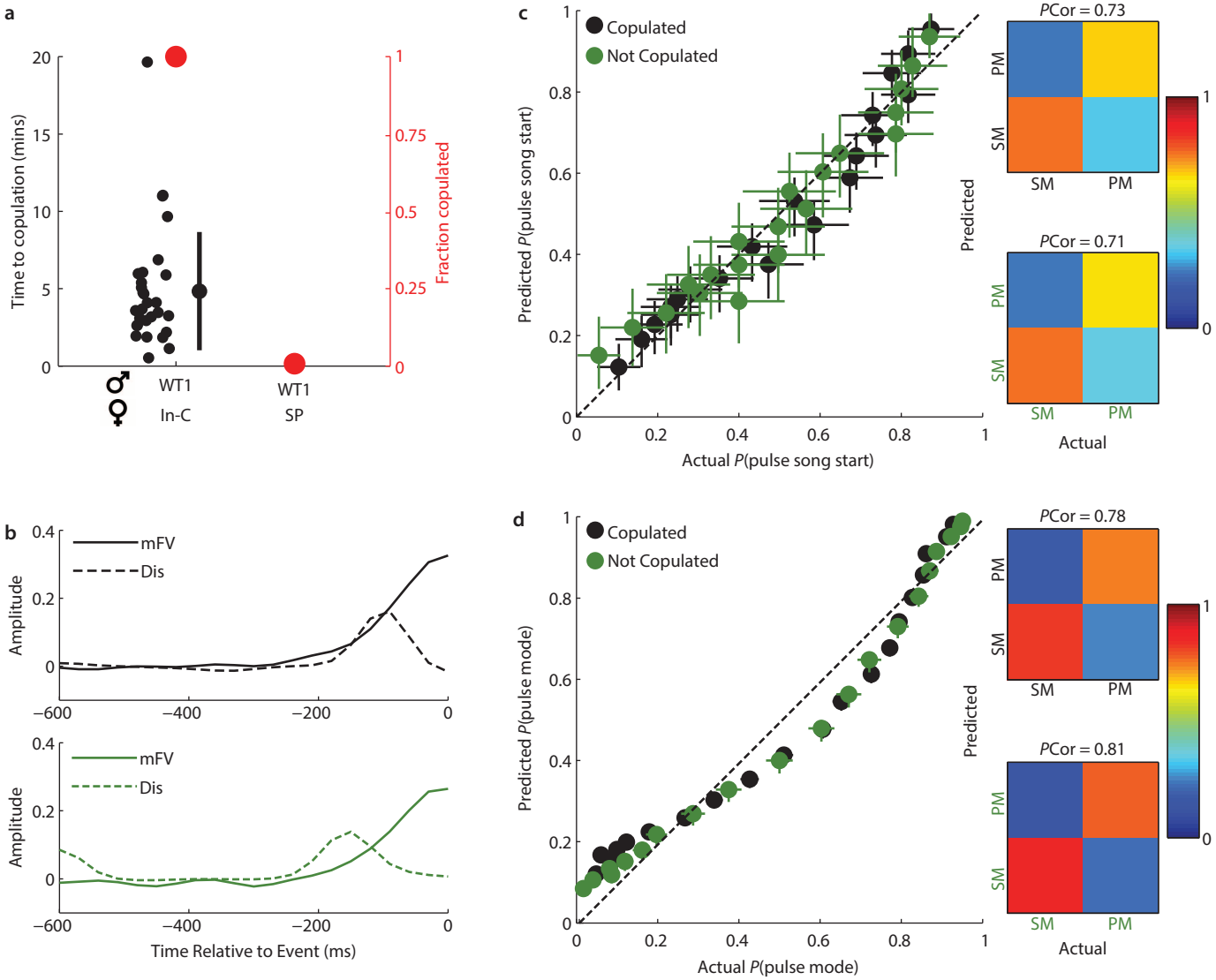

Extended Data Figure 7 | Failed copulations do not result from differences in song patterning decisions. **a,** Time to copulation (black) and fraction of copulating pairs (red) for sex-peptide-injected (SP) or control-peptide-injected (In-C) females paired with WT1 males ($n = 28$ or 30 males). Individual data points, mean and s.d. are given for In-C females (no SP females copulated). **b,** Male forward velocity (solid) and Dis (dashed) linear filters for song start classification (predicting songs that start in pulse mode versus sine mode). The GLM is based on data from wild-type flies that copulated (top, black) or did not copulate (bottom, green). **c,** GLM performance for classifying song starts with male forward velocity and Dis filters for wild type flies that copulated (black, *P*Cor = 0.72, $n = 2{,}490$ test events from 278 males) or did not copulate (green, *P*Cor = 0.71, $n = 1{,}458$ test events from 37 males). **d,** GLM performance for classifying current song mode (based on mean male forward velocity and male lateral speed) for wild-type flies that copulated (black, *P*Cor = 0.78, $n = 36{,}094$ test events from 278 males) or did not copulate (green, *P*Cor = 0.81, $n = 17{,}666$ test events from 37 males). Error bars indicate 95% confidence intervals, although some are too small to visualize (**c, d**).

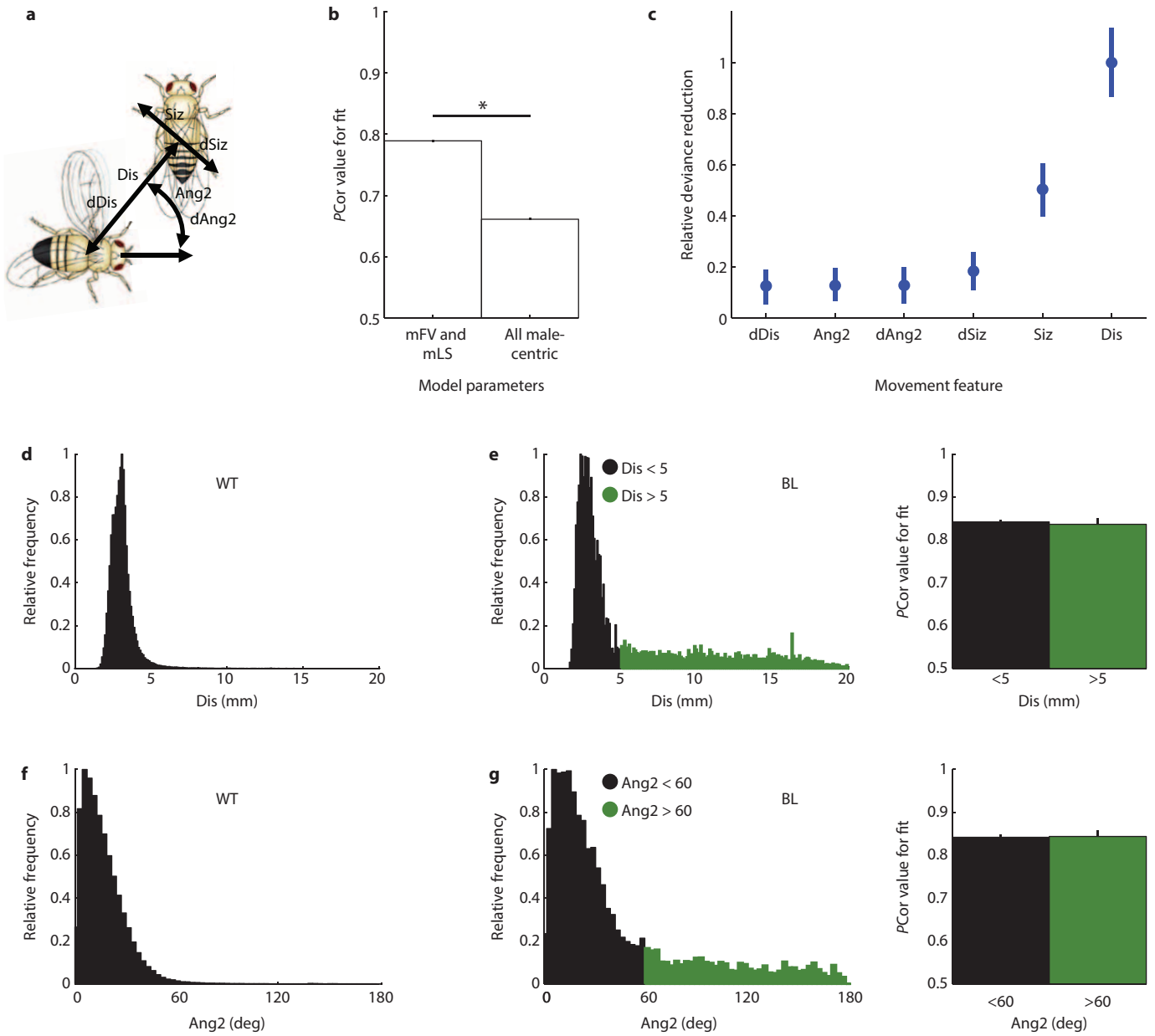

Extended Data Figure 8 | Male velocity consistently predicts the current mode of song. **a,** Male-centric features used to examine model performance. Dis and Ang2 are the same as described in Fig. 1a. Siz represents a projection of the female's body axis onto a plane perpendicular to a line joining the two fly centres (that is, the absolute value of the sine of the angle between female body axis and Dis). Thus, when Siz = 0 or 1, the female occupies a minimal or maximal region of the male's visual space respectively. dDis, dAng2 and dSiz represent the rate of change of Dis, Ang2 and Siz. **b,** Comparison of models to classify current song mode based on only male forward velocity and male lateral speed versus all 6 male-centric features combined (*$P < 0.001$). Models were tested using the same data set ($n = 55{,}464$ test events from 315 males). **c,** Deviance reduction statistics for models predicting song bouts starting in sine mode, using only male-centric features as inputs. Dis remains the most important feature (compare with Fig. 2). **d,** The distribution of Dis during song for wild-type males ($n = 338{,}238$ time points from 315 males). **e,** Left, the distribution of Dis during song for blind males ($n = 10{,}802$ time points from 33 males) is broader than for wild type. However, model performance (right) for GLMs using male forward velocity and male lateral speed to classify current song mode remains high for song samples produced at < 5 mm (black, $n = 2{,}074$ test events) or > 5 mm (green, $n = 650$ test events) from 33 males. **f,** As in **d**, but for Ang2 rather than Dis. **g,** As in **e**, but for Ang2 rather than Dis and splitting the data for Ang2 $< 60^\circ$ (black, $n = 2{,}258$ test events) or $> 60^\circ$ (green, $n = 534$ test events). Error bars indicate 95% confidence intervals, although some are too small to visualize (**b, c**, **e**, **g**).

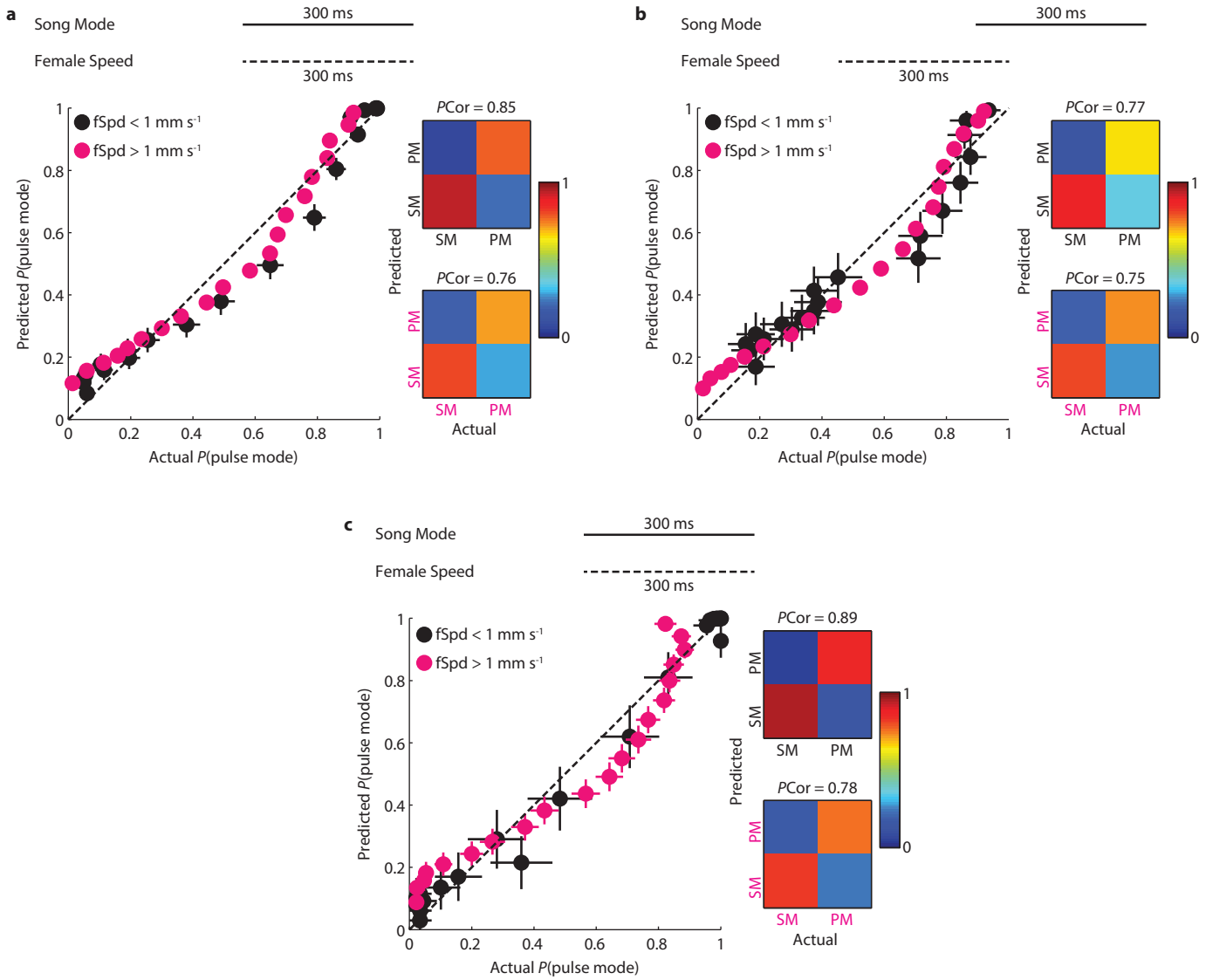

Extended Data Figure 9 | Models to predict current song mode during times when the female is stationary. **a,** GLM performance for classifying current song mode (based on mean male forward velocity and male lateral speed) for wild-type flies. The data set was divided into samples for which the female was effectively stationary during the song sample (black, *P*Cor = 0.85, $n = 9{,}454$ test events from 315 males), and those where she was moving (magenta, *P*Cor = 0.76, $n = 46{,}204$ test events from 315 males). Model performance remains high even without any motion cues from the female. **b,** As in **a**, but the data set is divided according to a shifted estimate of female speed, 240 ms before the song sample. This matches the most predictive region of the female BTA (Extended Data Fig. 3). Model performance remains high whether the female is stationary (black, *P*Cor = 0.77, $n = 3{,}110$ test events from 315 males) or moving (magenta, *P*Cor = 0.75, $n = 44{,}314$ test events from 315 males) 240 ms before the song sample. **c,** As in **a**, but using data from pheromone-insensitive males. Male velocity remains a successful predictor even when males cannot detect pheromones and when the female is stationary (black, *P*Cor = 0.89, $n = 1{,}788$ test events from 25 males) or moving (magenta, *P*Cor = 0.78, $n = 9{,}018$ test events from 25 males) during the song sample. Error bars in all plots indicate 95% confidence intervals, although some are too small to visualize.

Extended Data Table 1 | Descriptions and acronyms for all fly strains/genotypes

Acronym	Description
WT1	Wild type from Nairobi, Kenya; collected by Andolfatto & Bachtrog (2006)
WT2	Canton-S laboratory strain
WT3	Wild type from San Diego, California; collected by Andolfatto (2006)
WT4	Wild type from Cartagena, Colombia; collected by Andolfatto (2009)
WT5	Wild type from the Netherlands; collected by Davis (2000)
WT6	Wild type from Zanzibar, Tanzania; collected by Andolfatto & Bachtrog (2006)
WT7	Wild type from Harare, Zimbabwe; collected by Begun (1993)
WT8	Wild type from Victoria Falls, Zimbabwe; collected by Ballard (2002)
PI	Genetic manipulation to remove all volatile pheromone receptors and many general olfactory receptors
BL	Genetic manipulation to remove photoreceptors
PIBL	Genetic manipulation to remove photoreceptors and volatile pheromone receptors
AC	PIBL (female) or WT1 (male) flies had aristae removed > 20 hours before recording
WC	Male flies had wings removed > 20 hours before recording
SP	PIBL females injected with *Drosophila melanogaster* sex peptide 12-20 hours before recording
In-C	PIBL females injected with *Drosophila melanogaster* SIFamide peptide 12-20 hours before recording
oe^{-}	Genetic manipulation to remove pheromone producing cells (in PIBL females)
sim	*Drosophila simulans* strain from UCSD species stock center
Fru-A	Males expressing thermosensitive TrpA1 channels in all *fruitless* positive neurons.
Fru-B	Males expressing thermosensitive TrpA1 channels in all *fruitless* positive neurons, but with suppressed expression in the ventral nerve cord via the GAL80 system.
P1	Males expressing thermosensitive TrpA1 channels sparsely in putative song command (P1) neurons